



Seismic site characterization with shear wave (SH) reflection and refraction methods

James A. Hunter · Heather L. Crow · William J. Stephenson ·
André J.-M. Pugin · Robert A. Williams · James B. Harris ·
Jack K. Odum · Edward W. Woolery

Received: 3 February 2021 / Accepted: 18 August 2021 / Published online: 1 January 2022

This is a U.S. government work and not under copyright protection in the U.S.; foreign copyright protection may apply 2021

Abstract Reflection and critically refracted seismic methods use traveltimes of body waves propagating between a source and a series of receivers on the ground surface to calculate subsurface velocities. Body wave energy is refracted or reflected at boundaries where there is a change in seismic impedance, defined as the product of material density and seismic velocity. This article provides practical guidance on the

use of horizontally propagating shear wave (SH-wave) refraction and reflection methods to determine shear wave velocity as a function of depth for near-surface seismic site characterizations. Method principles and the current state of engineering practice are reviewed, along with discussions of limitations and uncertainty assessments. Typical data collection procedures are described using basic survey equipment, along with information on more advanced applications and emerging technologies. Eight case studies provide examples of the techniques in real-world seismic site characterizations performed in a variety of geological settings.

Article highlights

- A review of the principles and state-of-practice for shear wave refraction and reflection techniques for seismic site characterization.
- Guidance is provided on data collection and processing, along with information on technique limitations and uncertainty assessment.
- Eight case studies provide examples of shear wave surveys in various sedimentary settings, all in locations of elevated seismic hazard.

Keywords COSMOS guidelines · Seismic reflection · Seismic refraction · Shear wave velocity · V_{s30} · Seismic hazard · Seismic site characterization

J. A. Hunter · H. L. Crow · A. J.-M. Pugin
Geological Survey of Canada, Ottawa, ON, Canada

W. J. Stephenson (✉) · R. A. Williams · J. K. Odum
U.S. Geological Survey, Golden, CO, USA
e-mail: wstephens@usgs.gov

J. B. Harris
Department of Geosciences, Millsaps College, Jackson,
MS, USA

E. W. Woolery
Department of Earth and Environmental Sciences,
University of Kentucky, Lexington, KY, USA

The near-surface geological conditions at a site can have a significant impact on the amplitude and duration of seismic waves as they reach the surface. To reduce the effects of significant ground motion on structures, modern building codes worldwide have adopted seismic site classification schemes with categories that can be defined by the traveltimes-weighted average shear (S) wave velocity from ground surface to 30 m depth, referred to as V_{s30} . V_{s30} is an average velocity calculated by dividing 30 m by the traveltimes to that depth, as defined in the National Building Code of Canada (NRC 2010) and by the International Code Council (ICC 2015). This is different from the

root-mean square velocity (V_{RMS}), which is computed from the square root of the sum of the square of each layer's interval velocity multiplied by the transit time, divided by the sum of all the layer transit times. While many methods (direct and indirect, invasive and non-invasive) exist for the determination of S-wave velocities, this article addresses the non-invasive generation and recording of horizontally propagating S-waves (SH-waves) to calculate velocities directly from traveltime measurements of reflected and refracted waves.

The information in this article is founded on the reflection and refraction shear wave velocity measurement guidelines developed by the Geological Survey of Canada (GSC) in partnership with Canadian practitioners for seismic site characterization (Hunter and Crow, 2015). While the technique fundamentals remain relevant since this time, new emerging technologies, case studies, and updated references are provided herein.

1 Shear wave refraction

1.1 Introduction

In accordance with Snell's law, an elastic wavefront will be refracted when it encounters a boundary

between two materials with a seismic impedance contrast ($Z = \text{density} \times \text{velocity}$). The amplitude partition between reflected and refracted incident plane waves is predicted by the Zoeppritz (1919) equations. A nonplanar wavefront radiating from a point source will refract at the critical angle of incidence along the boundary and radiate energy back to the surface, yielding "head-wave" refractions (see Heelan 1953; Brekhovskikh 1960; Červený and Ravindra 1971). Velocity of, and depth to, the refracting surface can be calculated through traveltime measurements of the seismic wave between the seismic source and the receivers. Sample ray paths of refracted and reflected waves in some typical site conditions are shown in Fig. 1.

Seismic refraction methodologies for near-surface investigations were developed over 80 years ago (see Nettleton 1940; Jakosky 1950; Dobrin 1976). The American Society for Testing and Materials (ASTM) standard D5777-18 describes the methodology and equipment requirements for refraction surveying (ASTM D5777-18 2018). Most early near-surface, high-resolution refraction applications used compressional (P) waves generated by vertical impact weight drop or explosive sources and vertically polarized geophones. The refraction procedures discussed here employ a methodology similar to those described in ASTM D5777 for P-waves but instead use polarized S-waves radiating from horizontal

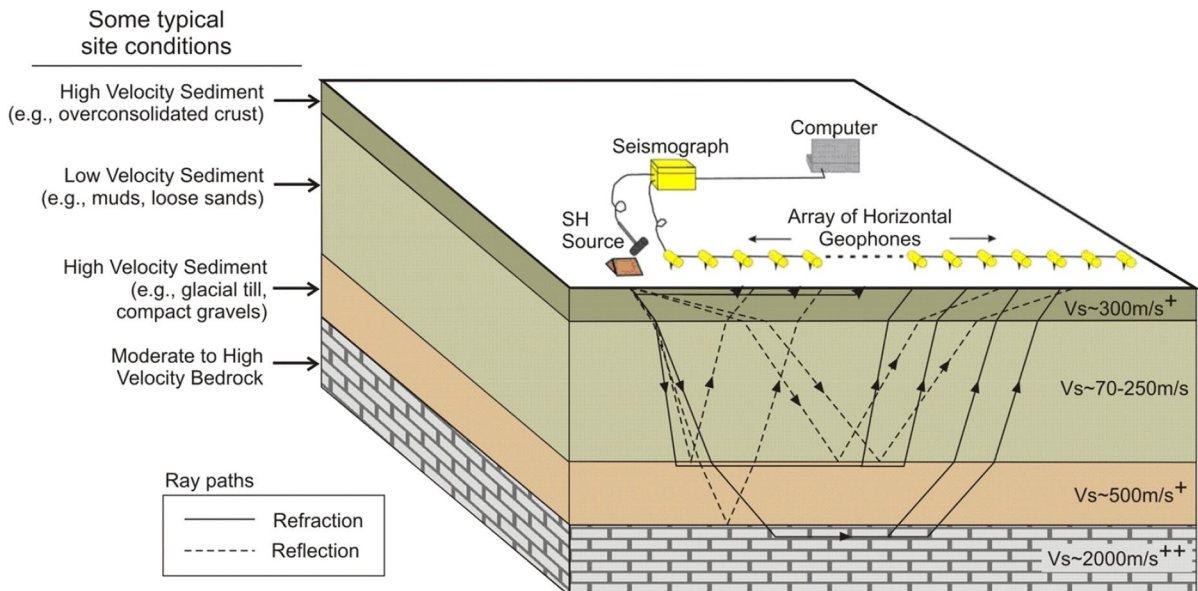


Fig. 1 Schematic of S-wave travel paths (reflected and refracted) through a typical sediment-over-bedrock setting. Figure modified from Hunter et al. (2015)

(SH) sources and horizontal geophones (Hunter et al. 1992, 1998a, b, 2002).

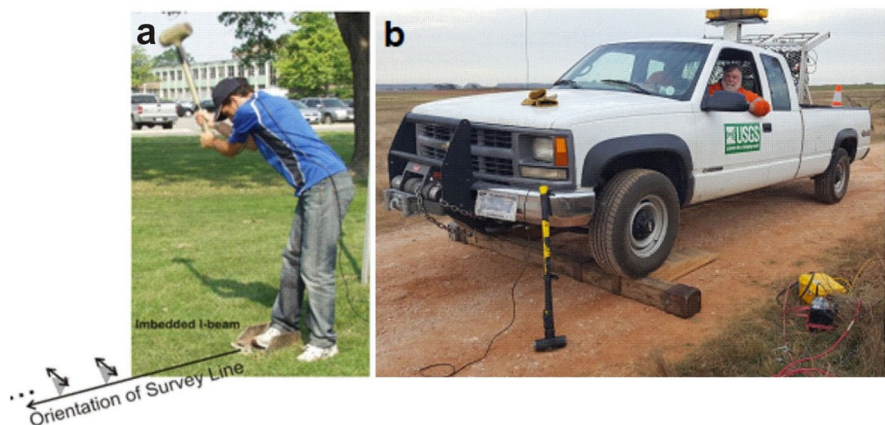
Shallow refraction techniques are subject to four notable limitations. First, as low-amplitude events, refractions may be difficult to identify in noisy environments where signal-to-noise (SN) ratios are low. Second, the presence of dipping subsurface layers may create significant variation in down-dip or up-dip apparent velocities, even for relatively low angles. Because dipping layers are extremely common, collecting forward and reverse shot positions for each geophone array is very important if site geometry allows. In settings with common sediment-bedrock velocity contrasts, Nettleton (1940) recommends that the calculated up- and down-dip velocities be averaged to estimate refractor velocities for dip angles of less than 20° . Third, refraction cannot reliably detect velocity reversals (or inversions), because the method is based on the assumption that each layer has a constant velocity and that these layer velocities increase with depth. In settings where higher velocity layers overlie lower velocity layers, other techniques (e.g., downhole shear, seismic cone penetrometer, multichannel analysis of surface waves) may be more appropriate. Finally, a layer must have a minimum thickness to be identified (Xia et al. 2002). This effect is referred to as the “blind zone” or “hidden layer” problem, and an example is given in Sect. 1.2. Generally, the ratio of the geophone array length to the refractor depth should be quite large (>5) to observe the first critically refracted arrival. In settings where softer sediments overlie a higher velocity rock or till (e.g., $Z > 20$), shorter arrays can be used, but this increases the possibility of the hidden layer problem.

1.2 Survey requirements

Refraction surveys require an array of relatively low frequency horizontal geophones (commonly 4.5 Hz or greater), a seismic cable to connect the geophones, a seismograph, field computer, and a seismic source with a triggering signal pulse (contract closure or pressure trigger). Most engineering seismographs have at least 12 input channels, and many instruments now offer 96 or more. One geophone is needed per channel, oriented transverse to the direction of the array. A 4.5- to 8-kg hammer striking a horizontally imbedded metal I-beam or weighted timber is generally a suitable source for shallow surveys (Fig. 2a, b). To reduce the potential for converted S- to P-wave interference that can occur if the source is struck in-line with the receivers, SH-polarized waves should be generated by striking the hammer at right angles to the direction of the array.

When selecting array parameters, the anticipated depth of investigation and velocity-depth distribution should guide the geophone spacing. In near-surface applications, 1- to 5-m separation is usually appropriate. As a minimum, shot locations are recommended at each end of the array and in center of the spread to obtain a pseudo-reversed-refraction record suite. Shots offset from the end of the array can be used in place of moving the geophone spread if the assumption of flat-lying subsurface layers is valid. To minimize unresolved static corrections, a true reversed refraction profile can be collected where the geophone location at each end of the array is replaced by a source location. For SH-refraction surveys, field records should be collected by hammering in one

Fig. 2 **a** I-beam and 7.3-kg hammer used as seismic source. Photograph by H.L. Crow. NRCan photo 2020–847. **b** Shear timber and 4.5-kg hammer. Photograph by W.J. Stephenson, U.S. Geological Survey



polarizing direction and then turning 180° to record a separate shot(s) in the opposite direction. Reverse polarity data at each shot position can assist with picking refraction arrival times during analysis. To improve the SN ratio and enhance the low-amplitude refractions from distant shot points, records from the same shot position may need to be digitally stacked in the field.

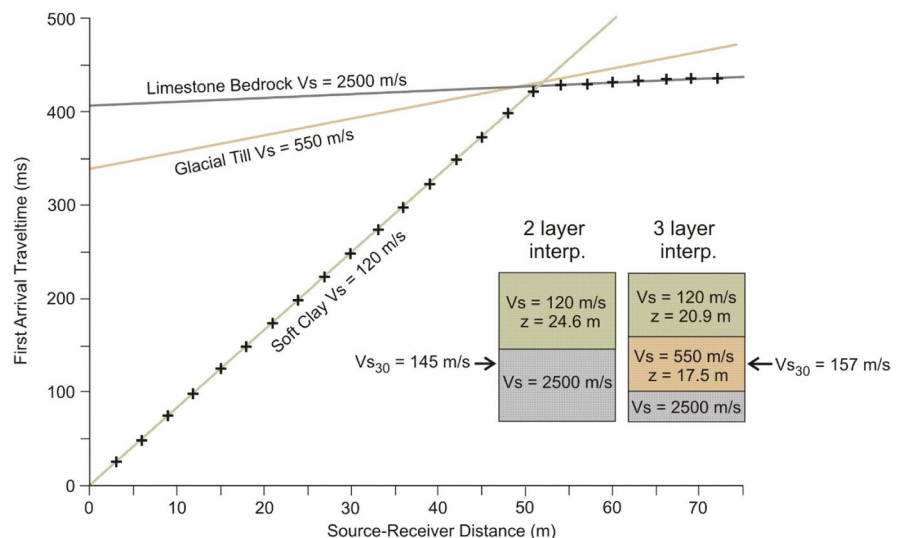
1.3 Data processing

The arrival time of shear wave energy can be analyzed using processing software available from many third-party vendors and open-source websites. ‘Time-distance’ plots are created by graphing traveltimes against the distance between the source and the geophones (Fig. 3). These plots are used to calculate an interval velocity for each of the refracting layers from the average of the forward and reverse plots using the inverse of the slope for each layer (see Case Study 1). The “intercept-time” method allows for the calculation of layer thicknesses from the velocities and intercept times of the slopes. The “critical distance” method can also be used to make layered interpretations. These and other methods are documented by Nettleton (1940), Musgrave (1967), Mooney (1984), Palmer (1988), Telford et al. (1990), and others. Software packages (see Sect. 2.2) are available to perform basic filtering, gain adjustments, pick arrival times, and interpret layer velocities and thicknesses. Refraction tomography techniques are becoming more

common (e.g., Sheehan et al. 2005). Tomographic methods do not require an assumption of continuous layers of constant velocity and are therefore useful in settings with varying velocity gradients and changing layer thicknesses.

When considering uncertainty in refraction processing, Williams et al. (2003a) estimated that a $\pm 10\%$ error on refraction velocity measurements is possible based on sensitivity analysis of refraction first break picking. Dipping or irregular layers, velocity reversals, velocity gradients, and lateral heterogeneity in shallow materials are all sources of uncertainty that influence the results of a velocity analysis using refraction methods. Site factors such as background noise levels, a sloping ground surface, practical limitations in array length, and coupling of source to ground surface also contribute to uncertainty. An interpreter also must be aware of interpretation complexities such as possible hidden layers, low-amplitude refractions, first arrival picking errors, and subtleties in selecting segments along the slope. To reduce the impact of these factors on data quality, forward and reverse shots in the field can help identify inclined or irregular layering. Stacking of recordings in the field can improve the identification of low-amplitude refractions. Data should be acquired at times when noise levels are acceptably low, defined here as a timeframe when the refraction signal is visibly as high as reasonable on test field records. Increasing the number of shots and receivers improves the definition of subsurface structure,

Fig. 3 Hypothetical forward time-distance plot showing the effect of an intermediate glacial till unit which could be undetected as a hidden layer. The variation in interpreted subsurface lithology is significant, and the resulting V_{s30} values are noted



allowing for more detailed interpretation routines that can better define lateral subsurface variability. Figure 3 presents the potential impact of the hidden layer problem, where a layer of intermediate velocity may be missed from first arrival time picking. In this example, a 17.5-m-thick layer of material with a V_s of 550 m/s would not produce a first arrival. An experienced interpreter may be able to identify the event from the presence of later arriving high-amplitude reflections.

When reporting on results for a shallow seismic site investigation, the equipment and survey parameters (e.g., geophone coordinates, frequency, and orientation) must be described along with any survey limitations (e.g., noise levels, line length restrictions, or array topography). Any information from nearby boreholes suggesting potential for velocity reversals or hidden layers should be described. Sample seismic field records should be included to indicate data quality. Interpretations of picked first arrivals of forward and reverse shots and the resulting time-distance plots with an error analysis of the slopes should be available for review in the report. Finally, the calculation of the average shear wave velocity to the depth of interest (V_{s30} or other) should be demonstrated in a table of interpreted layer thicknesses (z), velocities (V_s), and the calculated traveltime within each layer. Sample calculations are shown in Table 1.

1.4 Refraction case studies

1.4.1 Ottawa, Ontario, Canada: S-wave refraction in a seismic microzonation study

Between 2004 and 2011, the GSC and Carleton University collaborated in a microzonation project investigating the regional variation of soft sediment thickness and shear wave velocity across Canada’s National Capital Region (cities of Ottawa, Ontario, and Gatineau, Quebec). During the field program, seismic reflection and refraction data were collected at 750 test sites, and refraction events were visible on records at 527 of these sites. Key project outcomes were published of microzonation maps showing the distribution of seismic site classes and fundamental site periods across the region (Hunter et al. 2012; Motazedian et al. 2020).

The large impedance contrasts between the fine-grained soft sediment overlying the compact glacial

Table 1 Sample V_{s30} calculation from interpreted refraction layer velocities and thicknesses. The one-way traveltime within a given layer is calculated by dividing thickness by interval velocity. The total traveltime to the depth of interest (30 m in this example) was summed and divided into 30 to determine V_{s30}

Layer	Thickness (m)	Interval V_s (m/s)	Calculated travel time (s)	V_{s30} ($\sum z / \sum t$)
1	12	150	0.080	
2	6	600	0.010	
3	12	2700	0.004	
Sum	30		0.094	318

till or bedrock produced high-quality refraction (and reflection) records at many of the test sites (Hunter et al., 2010a). The stratigraphic sequence in the study area consisted of limestone, dolostone, shale, or granitic bedrock, overlain by thin glacial till deposits (average thickness ~7 m), capped by Holocene glaciomarine sediments composed of silt- and clay-size grains. Prior to identifying survey locations, surficial geology maps were consulted to select sites representing a range of near-surface materials. A sediment thickness map was also developed from a regional borehole database that provided guidance on survey design. A 3-m geophone separation was typically used, occasionally increased to 5 m in areas where soft sediments exceeded thicknesses of 100 m. Shot points were located at the center of the array and at off-end positions at 1, 1.5, and 10 times the geophone spacing. The selected source was a loaded metal I-beam struck with a 7.3-kg sledgehammer (Fig. 2a). Where bedrock was within 25–30 m of the surface, the 3-m array configuration with off-end shot points captured clear bedrock refractions (Fig. 4).

During data analyses, it was common to observe a high-velocity surface crust of either overconsolidated glaciomarine sediments or fill materials ($V_s = 250\text{--}400$ m/s), shown as the earliest arrivals of the near traces in Fig. 4. This high-velocity layer was approximately 1 to 5 m thick, and neglecting this layer had a limited effect on the interpretation of a traveltime-weighted average V_s interpretation to 30 m depth (V_{s30}) (Hunter et al. 2010a). The interpreted arrival times were exported from the picking software to produce traveltime-distance plots for forward and reverse shots (Fig. 5). The

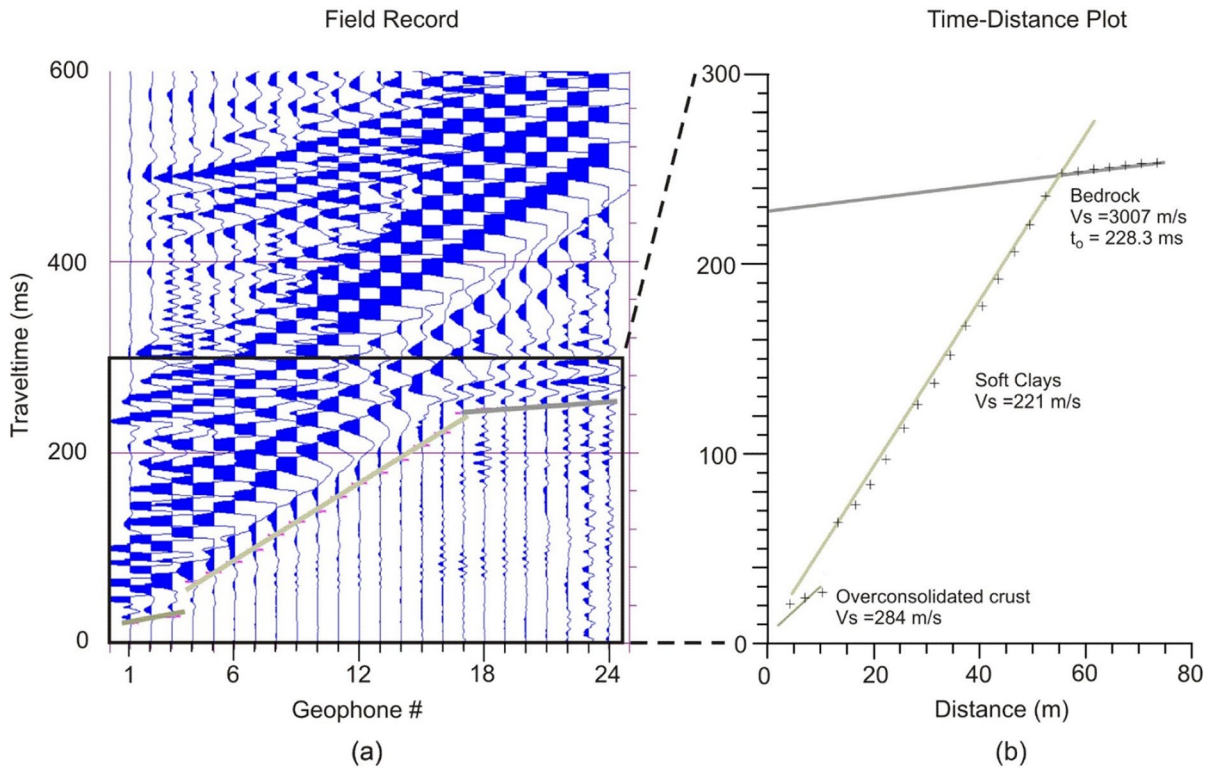


Fig. 4 **a** A single off-end shot record showing a thin, high-velocity surface crust, the refraction in the soft sediment, and the bedrock refraction. **b** The time-distance plot created from first arrival picks was used to interpret the interval velocity of each material

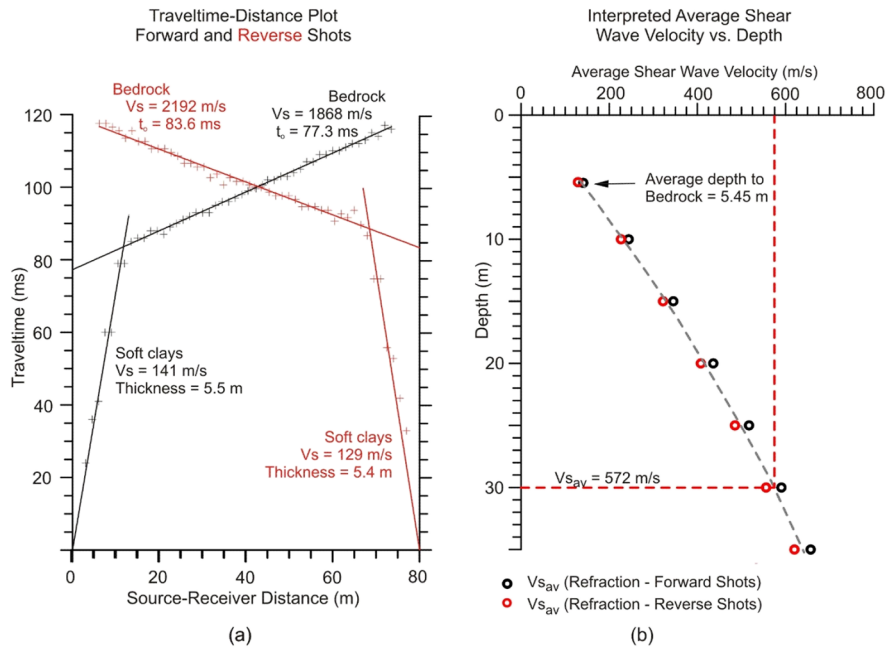
inverse of the slope was used to calculate the interval V_s for each material. Conventional “layered earth model” refraction interpretation methods (e.g., Telford et al. 1990) were used to calculate the thicknesses of the unit(s) above the bedrock. Differences between the forward and reverse bedrock velocities and time intercepts were interpreted as a dip along the bedrock surface. Forward and reverse bedrock velocities were averaged at sites where dip angles were interpreted to be less than 20° (Fig. 5). At rare sites where the dip was interpreted to be greater than 20° , the traveltime to the bedrock at the center of the array and the apparent velocities calculated at either end of the array were used to calculate a corrected sediment thickness at the array endpoints. This has the effect of deepening the up-dip sediment thicknesses and shallowing the down-dip thicknesses. In cases where site classes were found to be different at either end of the array, the lower of the two site classes was selected.

1.4.2 Fraser River Delta, British Columbia, Canada: S-wave refraction for earthquake hazard studies

The GSC collected and compiled shear wave surface (reflection, refraction) and borehole seismic data in the mid-1980s in the Fraser River Delta, British Columbia, to support regional earthquake hazard studies carried out by government, academic, and industry partners (Hunter et al. 1998a, 1998b). Refraction surveys were conducted at 112 sites using an array of 8-Hz geophones oriented in SH mode, with shot positions selected at either end of the array (Fig. 6a). A loaded I-beam was used as a source at sites where firm ground was within 40 m of the surface (e.g., Fig. 2a), and an 8-gauge in-hole shotgun was needed where sediment thickness exceeded 100 m.

Interpreted shear wave first arrivals from forward and reverse shots were exported to produce traveltime-distance plots (Fig. 6b). Two interpretation

Fig. 5 **a** Interpreted forward and reverse shot refraction arrivals on a time-distance plot showing intercept times, calculated S-wave velocities, and sediment thicknesses. Results indicate a relatively flat bedrock surface, allowing forward and reverse bedrock velocities to be averaged for the site. **b** Layer Vs and thickness results allow for the calculation of an average shear wave velocity down the bedrock for seismic site class calculations. Red and black open circles indicate the discrepancy between the forward and reverse interpretations



approaches were used to analyze the refraction datasets: the traditional “layer-case” method and the “velocity-depth” routine developed after Hunter (1971). The latter approach produced a running least-squares fit centered at each of the points on the traveltime-distance curve. This was seen as an advantage over the “layer-case” method which requires an interpreter to select straight line segments through the slope of the traveltime-distance points. The two techniques were shown to produce similar results (Figs. 6c, d), but the “velocity-depth” approach offers a more gradational increase in velocity with depth which is commonly associated with thick, near-surface, soft sediments.

1.4.3 San Fernando Valley, California, USA: S-wave refraction for seismic site effect investigations

The objective of the San Fernando Valley geophysical study was to investigate differences in shallow S-wave velocities at sites with varying amounts of building damage caused by the 1994 M6.7 Northridge earthquake (Fig. 7a; Williams et al. 1996). Due to generally limited space in this urbanized environment, array lengths ranged between 70 and 100 m for 11 sites, with example sites POT and MCK (shown in Fig. 7b) limited to 74-m offset. These data were collected with 24 14-Hz single-component geophones

separated by 3 m. A 4.0-kg sledgehammer striking a 15.2-cm-wide shear timber with metal endplates was used as the source (Fig. 2b). Source locations were at the array midpoint and endpoints with reversed polarity records collected at each location. The maximum depth of investigation at each site was estimated to be approximately 30 m based on the recommendation of Mooney (1984).

As described in Williams et al. (1996), the S-wave field records were first read into processing/analysis software and sorted by offset (source-to-receiver distance) so that the reversed polarity traces are overlain. The S-wave refraction arrivals in the seismic records were identified as the significant and laterally continuous polarity-reversed arrivals (Fig. 7b), which were then picked from the overlain records for each site. Williams et al. (1996) interpreted the refraction data using the slope-intercept method as described by Mooney (1984), which assumes continuous and possibly dipping layers across the length of the spread. Williams et al. (1996) averaged the resultant reflection and refraction depths to produce a one-dimensional depth-velocity profile that represents the site in the middle of the geophone spread. The seismic arrays were located on a generally flat surface; thus, no elevation corrections were needed (Williams et al., 1996).

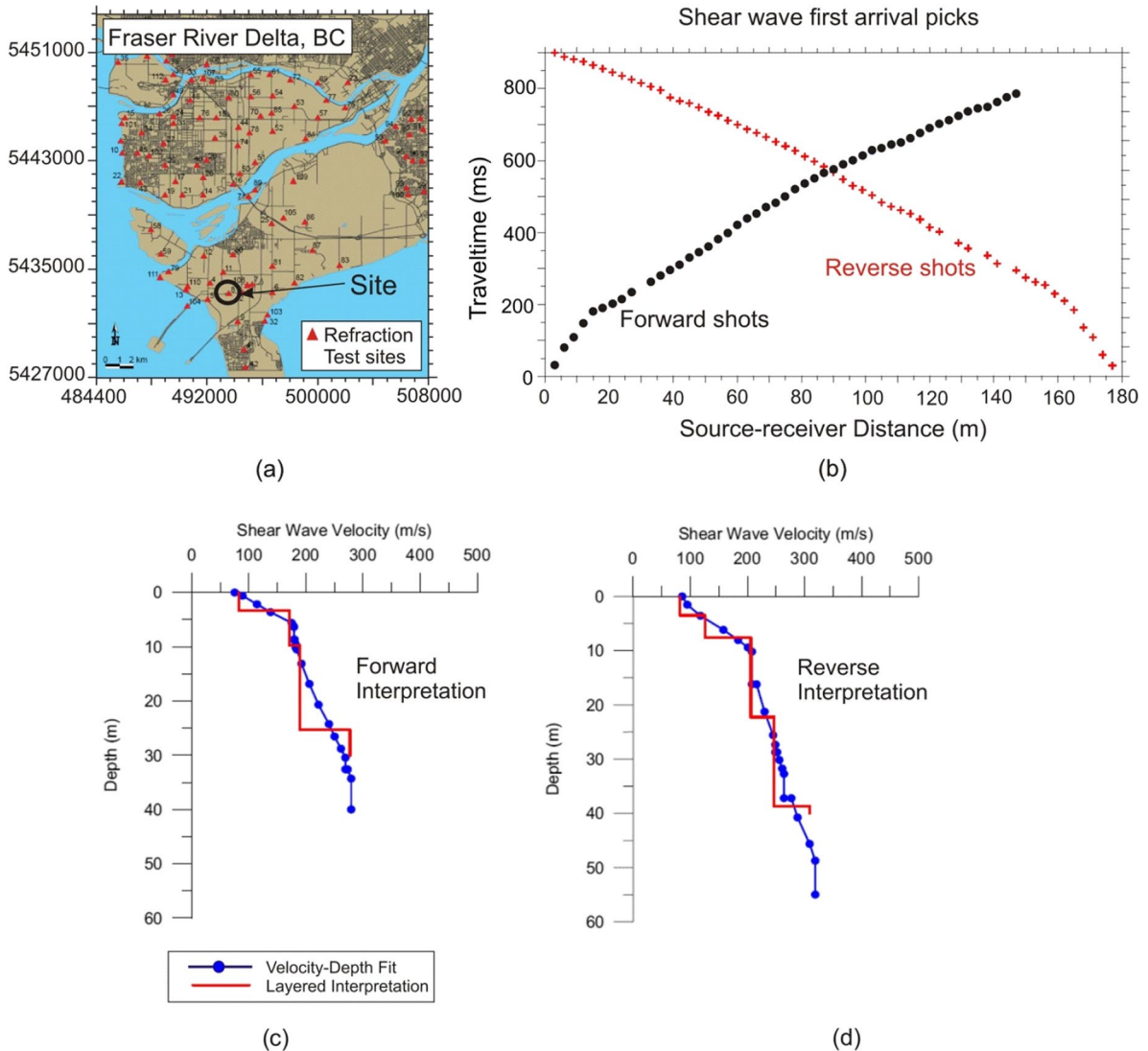


Fig. 6 Sample refraction survey data from the Fraser River Delta, British Columbia (Hunter et al. 1998a, 1998b). **a** Refraction data were acquired at 112 refraction sites throughout the study area. The location of the site shown in this figure is circled. **b** Traveltime-distance plot of the interpreted first arrivals of the forward and reverse shots. **c** and **d** Resulting

S-wave velocity-depth profiles, presented as layered interpretations and as “velocity-depth” fits using a routine developed by Hunter (1971). A 5-pt running least-squares fit is applied here along the traveltime-distance curve, yielding a continually varying velocity profile rather than the traditional single-velocity “layers.” Figure modified from Hunter et al. (2015)

2 Shear wave reflection

2.1 Introduction

Snell’s law and the Zoeppritz equations predict the partition of reflected and refracted energy when seismic waves encounter a boundary between two materials with a seismic impedance contrast

($Z = \text{density} \times \text{velocity}$) (e.g., Telford et al. 1990). Seismic reflection methods measure the time for seismic energy to travel down from a surface source to an impedance boundary and back up to receivers on the ground surface (Fig. 8). The shape of a traveltime curve from a reflection signal on a multi-receiver record is hyperbolic (Fig. 9) and can be used to calculate an average velocity from the ground surface to

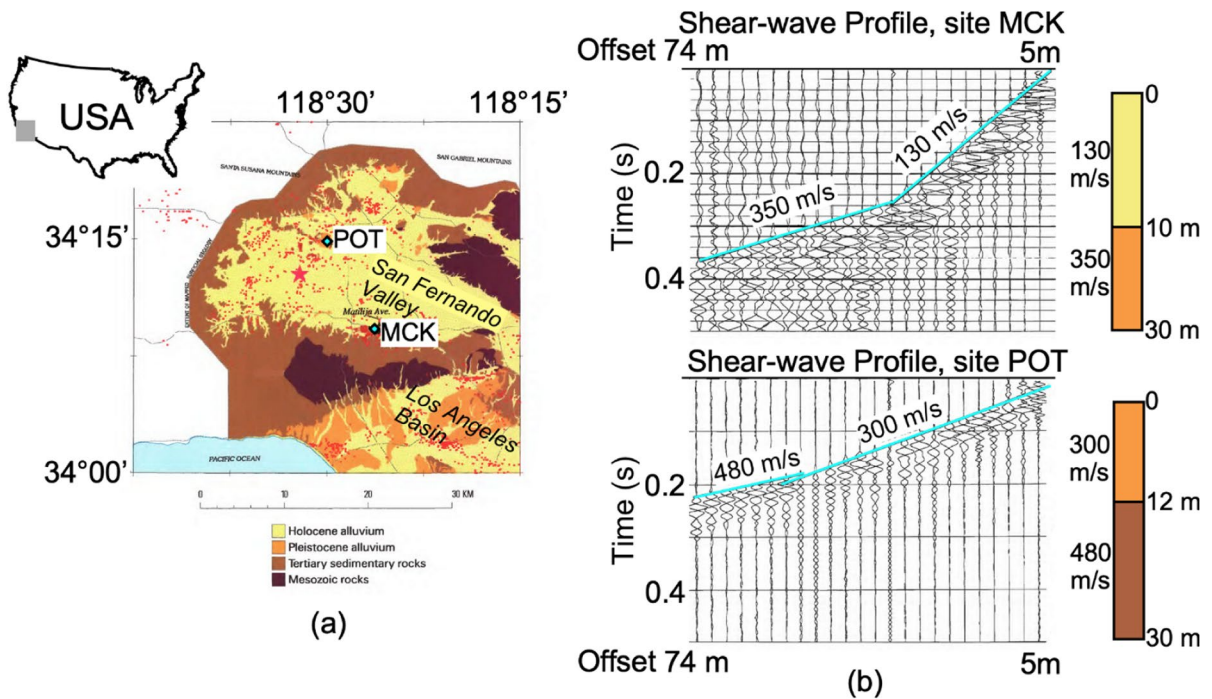


Fig. 7 **a** Generalized geologic map of the San Fernando Valley, CA, USA, with S-wave seismic refraction profiling sites POT and MCK shown. Red circles identify building locations made uninhabitable by the 1994 Northridge earthquake (epi-center at red star). Inset: gray box denotes proximal location of San Fernando Valley. **b** Interpreted SH-refraction records

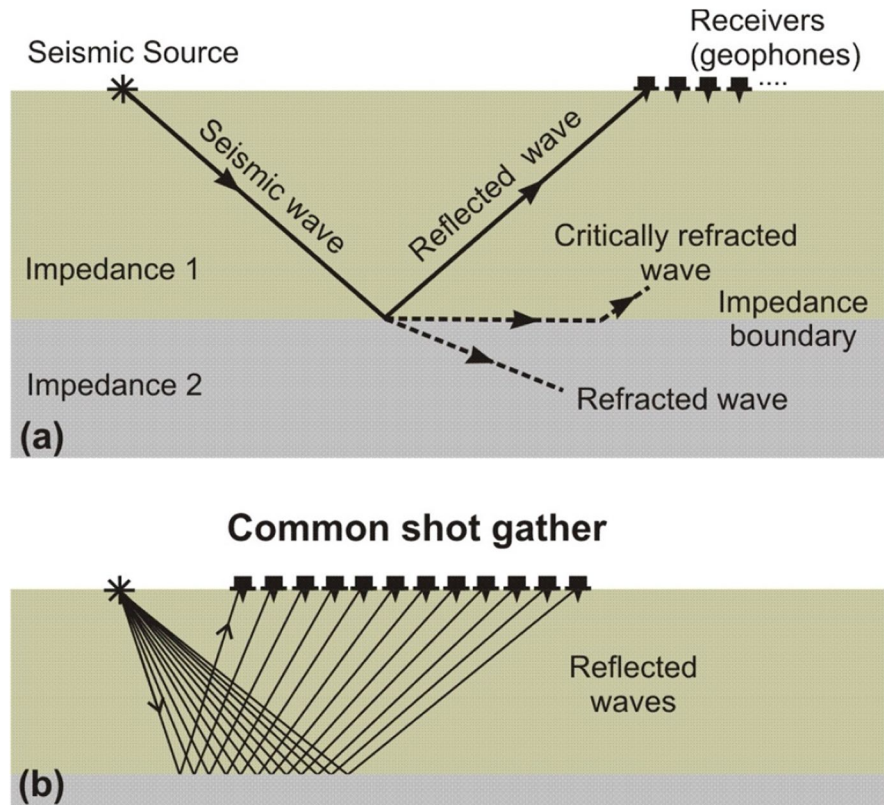
showing reversed polarity picking on traces displayed in “wiggle trace” mode. (Top) profile recorded in high damage area, and (bottom) record from an area of less damage. The reverse polarity display visually enhances refracted arrivals. Figure modified from Williams et al. (1996)

the reflecting horizon using the X^2 - T^2 method. For a flat-lying reflector, graphing the source-receiver distance squared (X^2) against the reflection arrival time squared (T^2) produces a plot with a slope equal to the inverse of the velocity squared (e.g., Telford et al. 1990). Reflection data can be collected using a single array of geophones or continuously collected along a longer survey alignment creating a two-way travel-time cross section of the subsurface. In this survey mode, the signal-to-noise (SN) ratio is improved by stacking data obtained with different source-receiver locations at the same common midpoint (CMP) (Fig. 10). The two-way traveltimes sections can then be converted into depth sections using either down-hole velocity logs from nearby borehole(s) or velocity-depth functions.

Deep seismic reflection has been a well-established technique in the oil exploration industry for many decades. Shallow reflection techniques were subsequently adapted in the 1980s when technological

advances allowed for portable engineering seismographs and field computers (Hunter et al. 1982, 1984; Doornenbal and Helbig 1983; Knapp and Steeples 1986b). The technique has been successfully applied in numerous shallow subsurface studies (e.g., Steeples and Miller 1990, 1998; Steeples 1998, 2005; Brouwer and Helbig 1998; Pullan and Hunter 1999; Brabham et al. 2005; Rabbel 2006) and developed into an ASTM standard (ASTM D7128-18 2018). Although seismic reflection surveys conventionally use compressional (P) waves, shallow S-wave reflection methods are also in practice. In unconsolidated materials, the velocity of P-waves is highly dependent on the degree of water saturation or the presence of gas, whereas S-waves are only sensitive to solid grains and are not transmitted through liquid. Because S-waves travel with lower velocities than P-waves, S-wavelengths are relatively shorter than P-wavelengths, often resulting in increased subsurface resolution (Helbig and Mesdag 1982; Stumpel et al.

Fig. 8 **a** Seismic waves generated on the ground surface travel from the source to an acoustic impedance boundary where they are partially refracted into the lower layer, and partially reflected back toward the surface. **b** Subsurface travel paths of reflections from a 12-channel field record. Figure modified from Pullan et al. (2015)



1984; Carr et al. 1998; Pugin et al. 2006). Therefore, shallow Vs reflection methods are highly useful for earthquake hazard studies (e.g., Woolery et al. 1993; Harris and Street 1997; Benjumea et al. 2003; Motazedian and Hunter 2008; Harris 2009, 2010; Hunter et al. 2010b; Odum et al. 2010). Shallow multicomponent reflection surveying recently is showing great potential (Pugin et al. 2009, 2010; Pugin and Yilmaz 2019) and is now being adopted into numerous projects with complex near-surface stratigraphy (e.g., Maries et al. 2017; Pugin et al. 2019).

As with refraction techniques, shallow reflection techniques are subject to limitations. First, to successfully resolve a survey target, it must be large relative to the wavelength (where wavelength is equal to the ratio of velocity over frequency) of the seismic signal. Second, near-surface materials, especially dry, high-porosity unconsolidated sediments, can strongly attenuate high-frequency energy. Thus, a major factor in determining survey quality and resolution is the ability to transmit high-frequency energy into the ground, which in turn depends on the near-surface materials,

the frequency and energy of the seismic source, the source-receiver spacings, and the coupling of the receivers and source with the ground. Noise levels also affect survey outcomes by reducing the SN ratio. Common sources include wind, local traffic, machinery operating nearby, and even interference from other types of seismic energy, like ground-coupled airwaves or surface waves (Miller et al. 1986). Finally, to calculate accurate velocities, the change in the arrival times of reflection events across the array (defined as the “moveout”) must be observed over a large range of source-receiver offsets. For a fixed array length, deeper reflections have a decreased moveout, resulting in reduced accuracy of velocity estimates with increasing depth.

2.2 Survey requirements

Shallow seismic reflection surveying requires a seismograph, geophones, multichannel cables to connect the array of receivers, and a seismic source connected to a highly accurate triggering unit. In

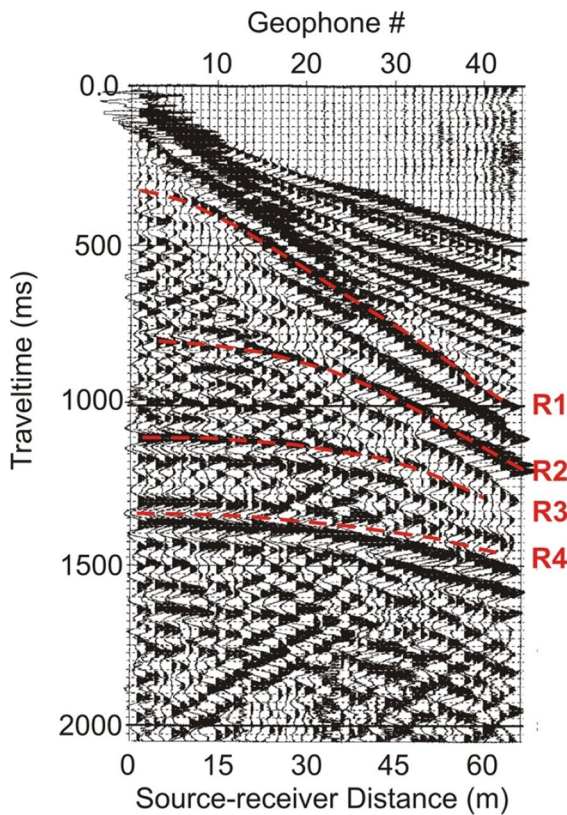


Fig. 9 Sample S-wave record collected in the Fraser River Delta. The shot record shows the hyperbolic nature of various reflected arrivals, noted as R1 to R4. The X^2-T^2 analysis of the arrival times from R4 yields an average shear wave velocity of 155 m/s down to this reflector at an estimated depth of 100 m. Data were obtained using 8-Hz horizontal geophones (stacked three times) and a 7.3-kg hammer striking a 15-kg I-beam. Figure modified from Pullan et al. (2015)

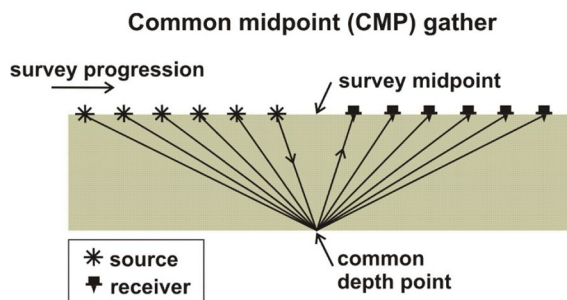


Fig. 10 Subsurface travel paths in a common midpoint (CMP) gather from six different field records. The traces will be processed together to produce one trace on the final seismic reflection section. The number of traces is referred to as the “fold” of the data. Figure modified from Pullan et al. (2015)

traditional applications, geophones are manually pushed into the ground, and the survey progresses by picking up and advancing (“rolling”) the cables and geophones down the line. Data are recorded at a series of shot positions along the array, and in this configuration, reflection and refraction data can often be collected together using a single array of receivers. The development of landstreamers has simplified this acquisition process by towing geophone arrays on sleds, an approach proven effective on roadways with motorized vehicles (e.g., Eiken et al. 1989; van der Veen and Green 1998; van der Veen et al. 2001; Inazaki 2004; Pugin et al. 2004, 2013).

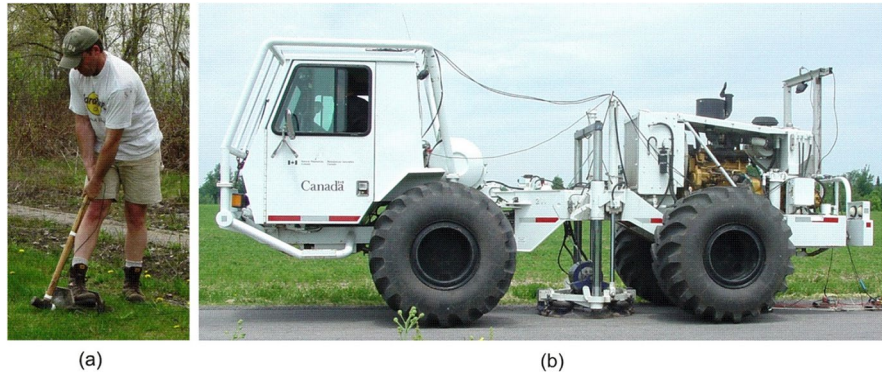
The seismic source also influences data quality, collection time, and thus, survey costs. Past comparisons between controlled seismic sources were carried out to study source attributes (Miller et al. 1992, 1994; Doll et al. 1998; van der Veen et al. 2000). Impulsive sources (e.g., sledgehammers, weight drops, explosives) are more traditional sources for shallow seismic surveys (Fig. 11a). Non-destructive vibratory sources (Fig. 11b) are heavy and relatively expensive but produce highly repeatable signals over a broad range of frequencies resulting in higher SN ratios in noisy settings (e.g., Pugin et al. 2013). In recent decades, small, lower cost vibratory sources have been designed for shallow seismic surveys (Ghose et al. 1998; Matsubara et al. 2002; Truskowski et al. 2004; Haines 2006; Pugin et al. 2020).

For a small survey with a single array, 12 to 96 geophones are typically set out, and records are collected using the same procedures described for refraction acquisition. In landstreamer applications, high-efficiency data collection is achieved as the source vehicle tows the receiver array and stops at a regular spacing to record data. For shallow surveys, the source-receiver spacing is generally on the order of a few meters, and receiver spacings are from sub-meter to meters.

2.3 Data processing

Several low-cost software programs are available to compute simple velocity and depth estimates from seismic reflection records using the X^2-T^2 method, which assumes a hyperbolic reflection event from a flat-lying reflector. Considerably, more processing

Fig. 11 Examples of S-wave seismic sources. **a** Sledgehammer hitting an I-beam coupled with the ground. **b** Large vibratory source. Photographs by A.J.-M. Pugin. NRCan photos 2020–848 and 2020–849



effort is required when using longer arrays of data to produce a seismic reflection section in two-way traveltimes. Data are sorted and grouped into common midpoint (CMP) gathers, a processing approach that improves the SN ratio by stacking a number of traces together with a range of source-receiver spacings. CMP processing requires a series of steps including trace editing, static corrections, filtering, gain scaling, velocity analyses, and normal moveout (NMO) corrections where each trace is corrected for offset according to a velocity-depth function determined from the data or from nearby borehole information. The NMO-corrected traces in each CMP gather are stacked together, producing one reflection trace for the final section. Once a section is created, surface topography adjustments can be applied, and the seismic time section can be converted to a depth section using velocity information. Specialized software is required to process seismic reflection profiles and can range from open-source code to programs costing thousands of dollars.

Two factors are critical when considering uncertainty in processed seismic reflection data: seismic wavelength and the SN ratio. Wavelength is the fundamental property affecting resolution, and thus the uncertainty in velocity and depth estimates. Under optimum conditions, S-wavelengths in near-surface soft sediments may be less than 1 m resulting in high-resolution sections, but typically, resolution is lower than this. Uncertainty will similarly increase when interpreting noisy data where the SN ratio is low. Noise can result from a combination of geological factors (e.g., near-surface material property variations creating “statics,” rough/steep reflecting horizons),

cultural (e.g., traffic, vibrations from machinery), or environmental effects (e.g., rain, wind).

The velocities and depths to reflectors interpreted from reflection data are also affected by uncertainties in arrival time picking of the wavelet, which may experience phase shifts with increasing offset and the assumption of hyperbolic moveout across the receiver spread. Slight overestimations of arrival times commonly occur when the peak or trough of the wavelet is picked rather than the exact shear onset. Errors in picking a consistent reflection signal across the record can also arise when changes in the source-receiver offset create phase shifts, resulting in velocity calculation errors. With careful picking or by estimating the picking delay, these effects can be identified. Finally, the accuracy of a velocity estimate using the X^2-T^2 method depends on the moveout of arrival times across the array. Uncertainty in velocity calculations can be reduced by increasing both the array length and number of geophones used in the array to improve the definition of the moveout. Using CMP gathers during analysis aids in the assumption of a hyperbolic moveout, but this assumption may be violated in some situations (e.g., refractive effects of a high-velocity surface layer resulting in non-hyperbolic traveltimes-distance plots), and velocity estimates generally become less accurate with increasing depth.

When reporting on survey results, digital records, commonly in SEG Y format (SEG Technical Standards Committee 2017), must be provided with field notes detailing instrumentation, recording parameters, geodetic coordinates of survey source and receiver locations if collected, and site conditions. A sample field record(s) should be included in a report

to indicate data quality and consideration of uncertainties in velocity estimates discussed above. Information about the software and the processing technique or steps followed must be provided with the final datasets.

2.4 Reflection case studies

2.4.1 Ottawa, Ontario, Canada: S-wave reflection in a seismic microzonation study

Between 2004 and 2011, the GSC and Carleton University collaborated in a microzonation project investigating the regional variation of soft sediment thickness and shear wave velocity across Canada’s National Capital Region. Project deliverables included regional V_{S30} and fundamental site period maps of the cities of Ottawa and Gatineau, Canada (Motazedian and Hunter 2008; Hunter et al. 2010a, 2010b, 2012; Motazedian et al. 2020). Fault-controlled bedrock basins produce rapid lateral changes in the thicknesses of fine-grained (silt and clay) post-glacial sediments that overlie thin glacial deposits and bedrock. Seismic reflection/refraction records collected at 750 sites around the cities were analyzed to produce average travelttime-weighted shear wave velocity-depth profiles, from which a seismic site class could be assigned.

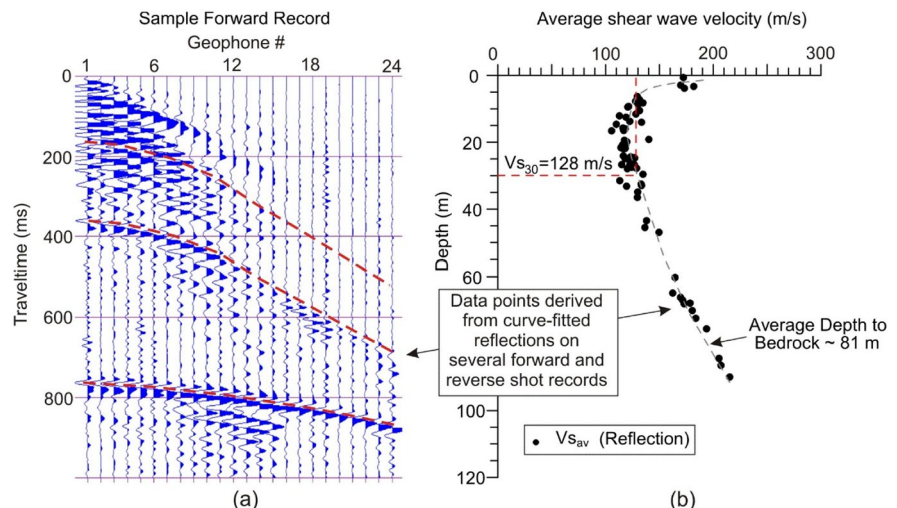
A 24-channel array of 4.5-Hz horizontal geophones oriented in horizontal shear (SH) mode was laid out at each site with either a 3- or 5-m spacing. A

4.5-kg hammer striking a steel I-beam with one edge dug into the ground in SH orientation was used as the seismic source (see Fig. 2a). Shot locations were at one and one-and-a-half geophone spacings off each end of the array, and one in the center of the array. This survey geometry allowed for trace-to-trace recognition of wide-angle reflections from the glacial or bedrock surface and provided enough source-geophone spacing to see bedrock refractions from depths up to 30 m. Where the postglacial sediments were thick, a bedrock refraction first arrival could not be detected. At these sites, only the reflections from the bedrock, glacial, and intra-sedimentary horizons were used to produce the site’s average velocity-depth profile (Fig. 12). Other researchers provide additional examples of the application of these techniques (Harris and Street 1997; Williams et al. 1999, 2003a, 2003b).

2.4.2 Fraser River Delta, British Columbia, Canada: S-wave profiling for seismic hazard modeling

The Fraser River delta in southwestern British Columbia is known to experience seismic wave amplification (Jackson et al. 2017), leading to greater levels of shaking during earthquakes. The delta’s location within the most seismically active region in Canada and the rapid population growth on the delta have raised concerns about the area’s seismic vulnerability. To aid in the assessment of earthquake hazards in the Fraser delta, seismic reflection surveys were carried out to image the structure of the delta

Fig. 12 Reflection records used to generate an average velocity-depth profile for V_{S30} assessment. The sample record shown in **a** is a forward shot from a deep (81 m) bedrock site, with several intra-sedimentary reflectors. **b** Time-averaged shear wave velocities were derived from hyperbolic curves fit to the reflections using seismic processing software



sediments (Pullan and Hunter 1987; Pullan et al. 1989). The depth to, shape of, and velocity contrast at the Holocene-Pleistocene boundary, defining the interface between younger, softer postglacial sediments and older, stiffer glacial till, were needed to model ground motion amplification in the delta.

Reflection profile alignments were selected near boreholes that intersected the Pleistocene boundary. Four S-wave reflection profiles were collected beneath the Arthur Laing Bridge, connecting Vancouver to the Vancouver International Airport on Sea Island. An array of 24 4.5-Hz horizontal geophones at 3-m spacings was used to record the data. The source was a 4.5-kg hammer striking an I-beam at an offset of 3 m from the end of the array. Profile Laing 1 is shown in Fig. 13. A strong reflector can be seen in the reflection profile, identified as the top of the Pleistocene till in borehole 90–1 located just beyond the southeast end of the profile (Hunter 1995). Other researchers have used S-wave reflection sections in earthquake hazard studies for the interpretation of near-surface faulting and sediment disturbance (e.g., Woolery et al. 1993, 1996; Woolery and Street 2002; Wang et al. 2003; Pullan et al. 2011; Brooks and Pugin 2019).

2.4.3 Ottawa, Ontario, Canada: S-wave profiling using landstreamer arrays in microzonation studies

The GSC routinely uses vibrating sources coupled with a multicomponent landstreamer receiver array to collect both P- and S-wave data at the same time (Pugin et al. 2009, 2013, 2020; Fig. 14a, b). With this acquisition system, it is possible to collect ~ 1000

multichannel records per day, an improvement many times beyond the hand-planting of geophones. In urban settings, the use of a vibratory source also provides greater stacking capability, resulting in less interference from wind or traffic noise.

Figure 15 shows a 1-km segment from an S-wave reflection profile that delineated a significant buried bedrock valley underneath a suburb of Ottawa, Ontario (Hunter et al. 2007). The section shows the shallow bedrock surface at the south end of the line, increasing in depth across two bedrock benches to a depth of nearly 90 m at the base of a buried escarpment. A nearby borehole confirmed the depths to the top of bedrock and a thin till layer that underlies the thick, soft, postglacial sediments. These soft sediments are associated with ground motion amplification that occurs during weak earthquake events recorded in the Ottawa area (Pugin et al. 2007; Khareshi Banab et al. 2012; Motazedian et al. 2020).

2.4.4 Combined shear wave refraction and reflection analyses

As geophysical methods continue to advance, the state of practice in shear wave site characterization will evolve toward full wavefield analysis. Numerous investigations have explored joint analysis of reflection and refraction traveltimes, but such methods are not used consistently in the state of practice today. In the following examples, simple approaches are used to compare and combine reflection and refraction traveltimes as a crosscheck for shear wave site characterization.

Fig. 13 S-wave reflection profile from the Fraser River delta showing a high-amplitude reflection at the top of the Pleistocene boundary. The velocity log from an off-section borehole (90–1) confirms the depth and V_s increase at the Pleistocene boundary. Figure modified from Pullan et al. (2015)

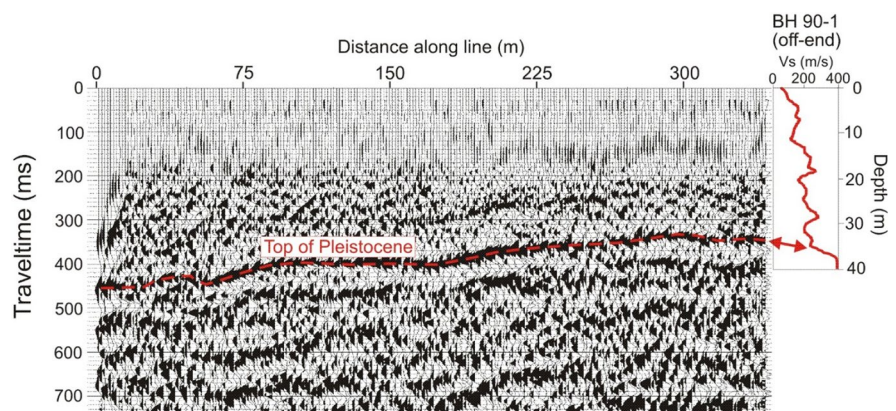


Fig. 14 Photos of GSC landstreamer systems in operation, Ottawa area, Canada. **a** Minivib source. **b** Microvibe source. Photographs by A.J.-M. Pugin. NRCan photos 2020–851 and 2020–850

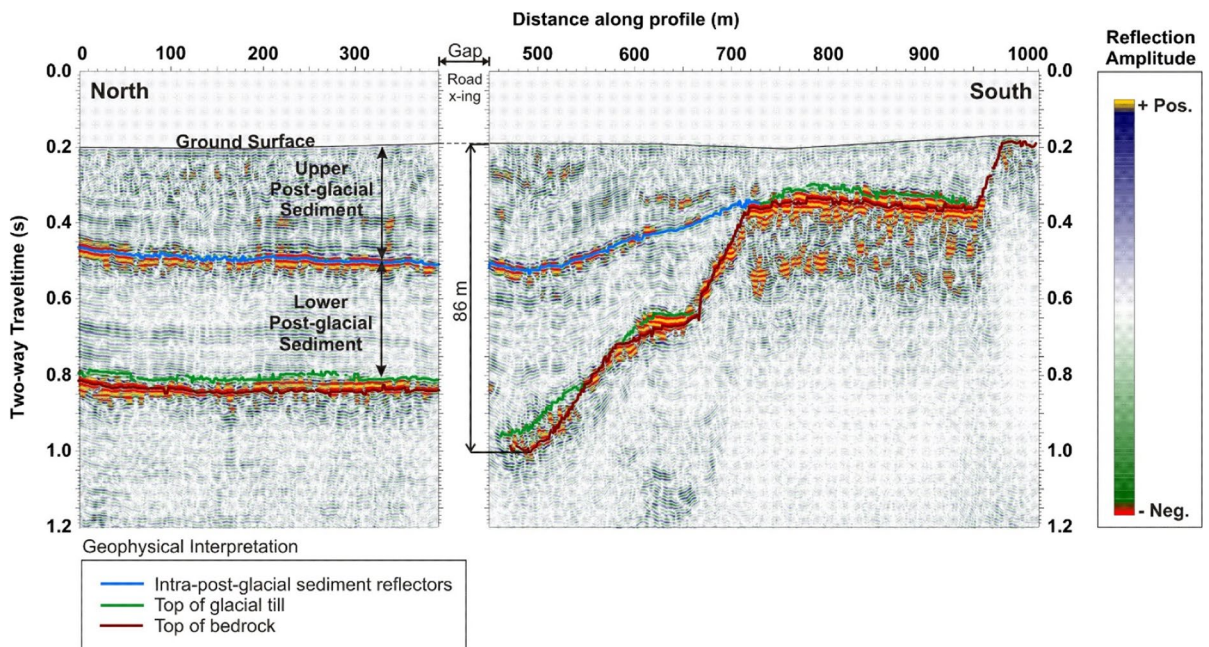
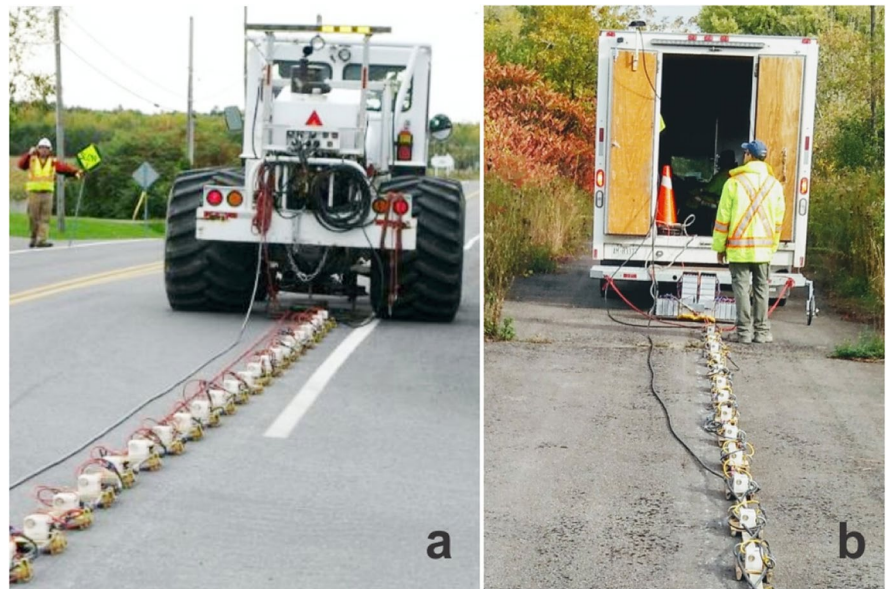


Fig. 15 A high-resolution S-wave reflection profile highlighting the structure within a buried bedrock valley in Ottawa, Ontario, Canada. The data were acquired along a busy street

with a Minivib source and a towed landstreamer array consisting of 24 channels at a 0.75-m spacing. Figure modified from Hunter et al. 2007

2.4.5 St. Louis, Missouri area, USA: S-wave data analyses for seismic site characterization

An example of a site characterization study in the central USA, where clear reflection and refraction

arrivals were recorded and independently interpreted, is shown in Fig. 16. These data were recorded on 4.5-Hz horizontal geophones spaced at 1.5 m with total source-receiver offsets from 0 to 120 m. A weighted shear timber (Fig. 2b) and 4.0-kg sledgehammer

provided the source energy. Williams et al. (2007) used the slope-intercept method as described by Williams et al. (1996) for interpreting these refraction data (Fig. 16). They interpreted the reflections using a reflection curve fitting application (in this case, a graphical X^2-T^2 analysis approach) commonly available in commercial engineering seismic data processing software. From the reflection curve fitting, the moveout velocities and zero-offset traveltimes were

picked and reflector depths were estimated using the Dix equation as described by Dobrin (1976). To get an estimate of the error bounds for both the reflection and refraction data, the interpreter can intentionally mis-position the line fit from the preferred slopes to a tolerable but extreme amount (Williams et al. 2003a). In this example, the maximum possible velocity variation is about 15% (see Williams et al. (2007)). Given the recorded dominant S-wave bandwidth of

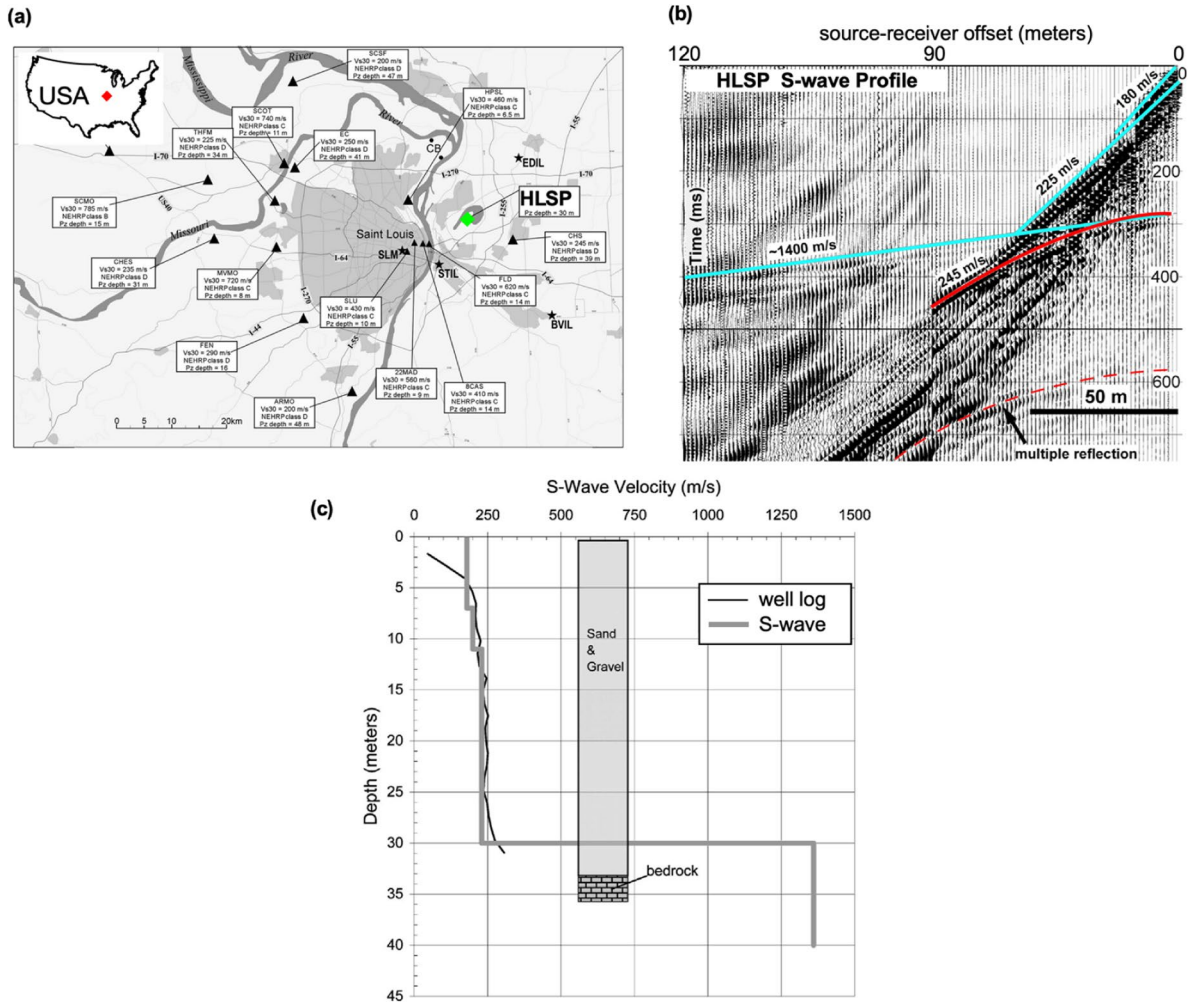
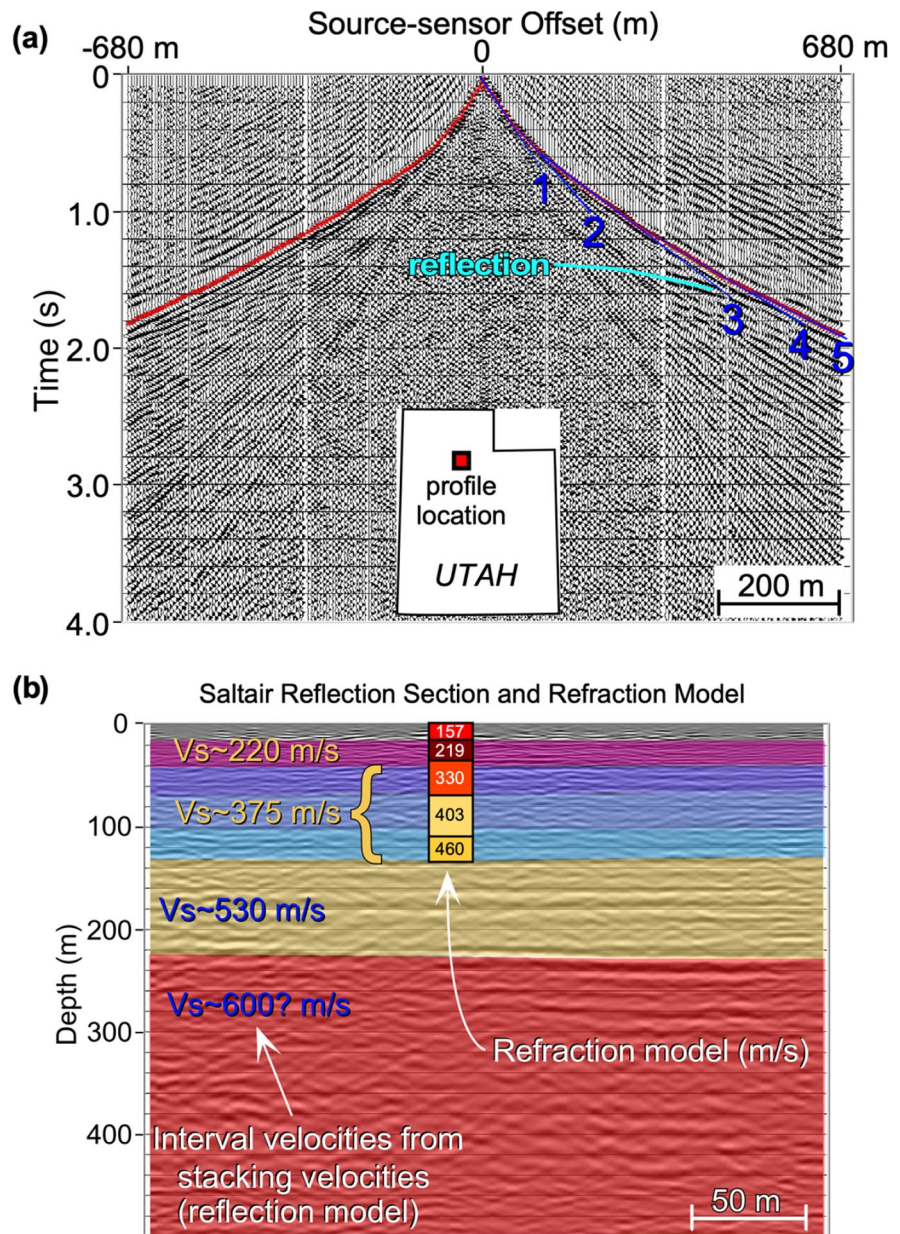


Fig. 16 **a** St. Louis, Missouri, metropolitan area with measurement sites (black triangles) described in Williams et al. (2007). Location of St. Louis shown by red diamond. Inset: site HLSP (green diamond) location in continental USA. **b** Unprocessed S-wave data of two 60-channel combined field records. First arrival refractions (cyan lines) indicate a prominent high-velocity (1,400 m/s) layer at far offsets, and solid red line is reflection arrival likely from same geologic interface, most likely bedrock. Dashed red line is a reflection multiple,

which could be misinterpreted as another event if interpreter does not recognize its zero-offset arrival time is twice that of the primary reflection. **c** Thin black line shows the downhole depth-velocity profile measured in a nearby borehole by the Illinois State Geological Survey. The refraction interpretation (heavy gray line) was developed without information from the well log. The reflection depth is estimated to be 34 m depth (shown by interpreted column in middle of graph). The interpreted bedrock depths differ by about 12%

Fig. 17 Example from Salt Lake Valley, Utah. **a** Traces from combined Minivib S-wave seismic records used for refraction interpretation, sorted by source-sensor offset distance. Refraction picks (red lines) and 5-layer interpretation (blue lines) are shown. Reflection labeled at 1.4 s (cyan line). Processing on refraction records included geometric sorting of selected records, gain correction, and bandpass filtering. Inset: site location within state of Utah (red square). **b** Common midpoint (CMP) reflection stack at site overlain by refraction model. Colored fill patterns on both reflection and refraction interpretations represent different geologic layers. The transparent color zones are interval velocities averaged over the intervals shown. Figure modified from Stephenson et al. (2007)



about 20–60 Hz and the interpreted seismic velocity structure, the resulting minimum vertical resolution is about 2 m, based on the quarter wavelength rule (Widess 1973).

2.4.6 Salt Lake Valley, Utah, USA: S-wave data analyses for seismic site characterization

In some geologic settings, S-wave site characterization can resolve velocity structure to depths

significantly greater than 30 m. An example of such an investigation is shown in Fig. 17. Here, Stephenson et al. (2007) used a Minivib source to acquire data at source-receiver offsets of up to 590 m in the Salt Lake Valley, Utah, where lake-bed deposits are favorable for such a deep sounding. These data were collected with 5-m station spacing and two 4.5-Hz single-component horizontal sensors at each of 59 stations over a 290-m array length. Using two sensors in this case improved the signal quality at far offsets

(Stephenson et al., 2007). Records were acquired at each end of the array and at 100-m intervals out to 300 m from the array ends. For reflection processing, additional records were acquired at every third station within the array to improve CMP coverage.

As detailed in Stephenson et al. (2007), the refraction arrivals were first picked and assigned to subsurface seismic layers in an initial refraction model based on traveltimes-offset analysis. A robust least-squares linear regression algorithm was then used to estimate intercept time and apparent refraction velocity for each picked layer. Finally, these intercept times and apparent velocities were modeled using the slope-intercept method to develop a “best” 1D refraction velocity model (Fig. 17a).

The reflection processing was conventional and included amplitude correction, filtering, and velocity analysis prior to the final stacked section. The stacking velocity field was converted to average-interval velocities based on prominent reflection locations in the stack. The resulting profile with the average-interval velocity field overprinted is shown in Fig. 17b, with the refraction model inset in the middle of the stacked section for comparison. Note that many of the refraction layers are imaged in the reflection data as well, and the average velocities of the models are in reasonable agreement. The maximum usable depth of the velocity model is roughly 225 m, based on the deepest prominent reflector depth.

3 Summary

A key option for seismic site category definition in modern building codes worldwide continues to be the traveltimes-weighted measurement of shear wave velocities to a depth of 30 m (V_{S30}). Non-invasive reflection and refraction techniques are used to directly characterize body wave velocities based on the measurement and analysis of traveltimes recorded at the ground surface. This article has demonstrated that the techniques are quite adaptable for shallow seismic site investigations, ranging from single-array surveys to more complex multi-array towed land-streamer surveys for high-impact projects or complex lithologies. Basic theory, equipment, survey configuration, data processing, limitations, and reporting requirements were discussed to support practitioners

in the standardization of the techniques for shallow seismic site classification surveys.

While surface wave methods have gained prominence in site characterization over the past several decades, body waves provide important constraints on subsurface wave speed and wave propagation effects unique from those inferred from surface waves, which often require inverse modeling to obtain shear wave velocity from phase velocity. As the state-of-practice of seismic site characterization continues to evolve, including implementation of full waveform inversion, body wave methods will need to play a critical role in that evolution.

Acknowledgements The Consortium of Organizations for Strong Motion Observation Systems (COSMOS) consisting of the US Geological Survey, the Geological Survey of Canada (GSC), and a group of North American power companies, consisting of Southern California Edison and Pacific Gas and Electric, identified the need for these blind trials, for these guidelines for best-practices and provided funding and encouragement to facilitate the project. This material is also based upon work supported by the US Geological Survey under Cooperative Agreement No. G17AC00058. The views and conclusions contained in this document are those of the authors and should not be interpreted as representing the opinions or policies of the US Geological Survey. Mention of trade names or commercial products does not constitute their endorsement by the US Geological Survey. Any use of trade, product, or firm names is for descriptive purposes only and does not imply endorsement by the US Government, the Canadian Government, or COSMOS. This paper is Natural Resources of Canada contribution number 20200665.

Open Access publication fees for this paper were directly funded by GSC.

Funding for investigations in Canada was provided by the GSC Public Safety Geoscience Program and the Natural Sciences and Engineering Research Council. This article represents GSC contribution number 20200677. Funding for investigations in the USA was provided by the U.S. Geological Survey (USGS) Earthquake Hazards Program.

The authors gratefully acknowledge numerous project participants in the case studies. The GSC authors thank Kevin Brewer, Greg Brooks, Robert Burns, Tim Cartwright, Ron Good, Dariush Motazedian, Matt Pyne, Susan Pullan, and many student contributors. The USGS authors thank David Worley (USGS, retired) for his valuable contributions to the US investigations presented in this manuscript. We thank Alena Leeds, two anonymous reviewers, and Guest Editor John Cassidy for their suggestions and insights that improved this manuscript.

Funding Funding for investigations in Canada was provided by the Geological Survey of Canada’s (GSC) Public Safety Geoscience Program and the Natural Sciences and Engineering Research Council. This article represents GSC contribution number 20200677. Funding for investigations in the USA was provided by the U.S. Geological Survey (USGS) Earthquake Hazards Program.

Code availability N/A

Declarations

Conflict of interest The authors from the GSC and the U.S. Geological Survey have no conflicts of interest to declare. Any use of trade, firm, or product names is for descriptive purposes only and does not imply endorsement by the U.S. or Canadian Governments.

Open Access This article is licensed under a Creative Commons Attribution 4.0 International License, which permits use, sharing, adaptation, distribution and reproduction in any medium or format, as long as you give appropriate credit to the original author(s) and the source, provide a link to the Creative Commons licence, and indicate if changes were made. The images or other third party material in this article are included in the article's Creative Commons licence, unless indicated otherwise in a credit line to the material. If material is not included in the article's Creative Commons licence and your intended use is not permitted by statutory regulation or exceeds the permitted use, you will need to obtain permission directly from the copyright holder. To view a copy of this licence, visit <http://creativecommons.org/licenses/by/4.0/>.

References

- ASTM D5777-18 (2018) Standard guide for using the seismic refraction method for subsurface investigation, ASTM International, West Conshohocken, PA. <https://doi.org/10.1520/D5777-18>
- ASTM D7128-18 (2018) Standard guide for using the seismic-reflection method for shallow subsurface investigation, ASTM International, West Conshohocken, PA. <https://doi.org/10.1520/D7128-18>
- Benjumea B, Hunter JA, Aylsworth JM, Pullan SE (2003) Application of high-resolution seismic techniques in the evaluation of earthquake site response, Ottawa Valley, Canada. In: McBride JH and Stephenson WJ (eds) Contributions of High Resolution Geophysics to Understanding Neotectonic and Seismic Hazards. *Tectonophysics* 368:193–209. [https://doi.org/10.1016/S0040-1951\(03\)00158-6](https://doi.org/10.1016/S0040-1951(03)00158-6)
- Brabham PJ, Thomas J, McDonald RJ (2005) The terrestrial shallow seismic reflection technique applied to the characterization and assessment of shallow sedimentary environments. *Q J Eng GeolHydrogeol* 38:23–38. <https://doi.org/10.1144/1470-9236/04-300>
- Brekhovskikh LM (1960) Waves in Layered Media. In: Frenkiel FN and Temple G (eds) Applied Mathematics and Mechanics vol 6. Academic Press, New York. <https://doi.org/10.1002/zamm.19620420308>
- Brooks GR, Pugin AJ-M (2019) Assessment of a seismo-neotectonic origin for the New Liskeard-Thornloe scarp, Timiskaming Graben, northeastern Ontario. *Can J Earth Sci.* <https://doi.org/10.1139/cjes-2019-0036>
- Brouwer J, Helbig K (1998) Shallow high-resolution reflection seismics. In: Helbig K, Treitel S (eds) Handbook of Geophysical Exploration 19 Elsevier Science Ltd, Amsterdam.
- Carr BJ, Hajnal Z, Prugger A (1998) Shear-wave studies in glacial till. *Geophysics* 63:1273–1284. <https://doi.org/10.1190/1.1444429>
- Červený V, Ravindra R (1971) Theory of seismic head waves. University of Toronto Press, Toronto. <https://doi.org/10.3138/9781442652668>
- Dobrin MB (1976) Introduction to geophysical prospecting. McGraw-Hill, New York
- Doll WE, Miller RD, Xia J (1998) A noninvasive shallow seismic source comparison on the Oak Ridge Reservation, Tennessee. *Geophysics* 63:1318–1331. <https://doi.org/10.1190/1.1444433>
- Doornenbal JC, Helbig K (1983) High-resolution shallow seismics on a tidal flat in the Dutsch Delta- acquisition, processing and interpretation. *First Break* 1:9–20. <https://doi.org/10.3997/1365-2397.1983010>
- Eiken O, Degutsch M, Riste P, Rød K (1989) Snowstreamer: an efficient tool in seismic acquisition. *First Break* 7:374–378. <https://doi.org/10.3997/1365-2397.1989021>
- Ghose R, Nijhof V, Brouwer J, Matsubara Y, Kaida Y, Takahashi T (1998) Shallow to very shallow, high-resolution reflection seismic using a portable vibrator system. *Geophysics* 63:1295–1309. <https://doi.org/10.3997/1365-2397.1989021>
- Haines SS (2006) Design and application of an electromagnetic vibrator seismic source. *J Environ Eng Geophys* 11:9–15. <https://doi.org/10.2113/JEEG11.1.9>
- Harris JB (2009) Hammer-impact, SH-wave seismic reflection methods in neotectonic investigations: General observations and case histories from the Mississippi Embayment, U.S.A. *J Earth Sci* 20:513–525. <https://doi.org/10.1007/s12583-009-0043-y>
- Harris JB (2010) Application of shallow shear-wave seismic reflection methods in earthquake hazard studies. *Lead Edge* 29:960–963. <https://doi.org/10.1190/1.3480010>
- Harris JB, Street RL (1997) Seismic investigation of near-surface geological structure in the Paducah, Kentucky, area: application to earthquake hazard evaluation. *Eng Geol* 46:369–383. [https://doi.org/10.1016/S0013-7952\(97\)00012-4](https://doi.org/10.1016/S0013-7952(97)00012-4)
- Heelan PA (1953) On the theory of headwaves. *Geophysics* 18:871–893. <https://doi.org/10.1190/1.1437941>
- Helbig K, Mesdag CS (1982) The potential of shear-wave observations. *Geophys Prospect* 30:413–431. <https://doi.org/10.1111/j.1365-2478.1982.tb01314.x>
- Hunter JA (1971) A computer method to obtain the velocity-depth function from seismic refraction data. In: Report of Activities, Part B, Geological Survey of Canada Paper 71-1B, pp 40–48. <https://doi.org/10.4095/105472>
- Hunter JA, Burns RA, Gagne RM, Good RL, MacAulay HA (1982) Mating the digital engineering seismograph with the small computer - some useful techniques. In: Current Research, Part B, Geological Survey of Canada, Paper 82-1B, pp 131–139. <https://doi.org/10.4095/119325>
- Hunter JA, Pullan SE, Burns RA, Gagne RM, Good RL (1984) Shallow seismic reflection mapping of the overburden-bedrock interface with the engineering seismograph - some simple techniques. *Geophysics* 49:1381–1385. <https://doi.org/10.1190/1.1441766>
- Hunter JA, Luternauer JL, Neave KG, Pullan SE, Good RL, Burns RA, Douma M (1992) Shallow shear wave

- velocity-depth data in the Fraser Delta from surface refraction measurements, 1989, 1990, 1991. Geological Survey of Canada, Open File 2504. <https://doi.org/10.4095/133371>
- Hunter JA (1995) Shear wave velocities of Holocene sediments, Fraser River delta, British Columbia. Geological Survey of Canada, Current Research 1995-A, pp 29–32. <https://doi.org/10.4095/202754>
- Hunter JA, Burns RA, Good RL, Pelletier CF (1998a) A compilation of shear wave velocities and borehole geophysics logs in unconsolidated sediments of the Fraser River Delta, British Columbia. Geological Survey of Canada, Open File 3622. <https://doi.org/10.4095/298718>
- Hunter JA, Douma M, Burns RA, Good RL, Pullan SE, Harris JB, Luternauer JL, Best ME (1998b) Testing and application of near surface geophysical techniques for earthquake hazards studies, Fraser River Delta, British Columbia. In: Clague JJ, Luternauer JL, Mosher DC (eds) *Geology and Natural Hazards of the Fraser River Delta*, British Columbia. Geological Survey of Canada Bulletin 525, pp 123–145. <https://doi.org/10.4095/210031>
- Hunter JA, Benjumea B, Harris JB, Miller RD, Pullan SE, Burns RA, Good RL (2002) Surface and downhole shear wave seismic methods for thick soils site investigations. *Soil Dyn Earthq Eng* 22:931–941. [https://doi.org/10.1016/S0267-7261\(02\)00117-3](https://doi.org/10.1016/S0267-7261(02)00117-3)
- Hunter JA, Motazedian D, Pugin AJ-M, Khasheshi-Banab K (2007) Near surface geophysical techniques for mapping soft soil earthquake shaking response within the City of Ottawa, Canada. In *Proceedings: Society of Exploration Geophysicists Annual Meeting*, San Antonio, TX, pp 1118–1122 (expanded abstract). <https://doi.org/10.1190/1.2792603>
- Hunter JA, Crow HL, Brooks GR, Pyne M, Lamontagne M, Pugin AJ-M, Pullan SE, Cartwright T, Douma M, Burns RA, Good RL, Motazedian D, Khasheshi-Banab K, Caron R, Kolaj M, Folahan I, Dixon L, Dion K, Duxbury A (2010a) Seismic site classification and site period mapping in the Ottawa area using geophysical methods. Geological Survey of Canada, Open File 6273. <https://doi.org/10.4095/286323>
- Hunter JA, Burns RA, Good RL, Pullan SE, Pugin AJ-M, Crow HL (2010b) Near-surface geophysical techniques for geohazard investigations: some Canadian examples. *Lead Edge* 29:936–947. <https://doi.org/10.1190/1.3480011>
- Hunter JA, Crow HL, Brooks GR, Pyne M, Lamontagne M, Pugin AJ-M, Pullan SE, Cartwright T, Douma M, Burns RA, Good RL, Motazedian D, Khasheshi-Banab K, Caron R, Kolaj M, Muir D, Jones A, Dixon L, Plastow G, Dion K, Duxbury A (2012) Ottawa-Gatineau seismic site classification map from combined geological/geophysical data. Geological Survey of Canada, Open File 7067. <https://doi.org/10.4095/291440>
- Hunter JA, Crow HL (2015) Shear wave velocity measurement guidelines for Canadian seismic site characterization in soil and rock. *Earth Sci Sect Gen Inf Prod* 110e. <https://doi.org/10.4095/297314>
- Hunter JA, Crow HL, Schmok J (2015) Shear wave refraction technique for hazard studies. In: Hunter JA, Crow HL (eds) *Shear Wave Velocity Measurement Guidelines for Canadian Seismic Site Characterization in Soil and Rock*. Geological Survey of Canada, Earth Science Sector, General Information Product 110 e, p.22–33. <https://doi.org/10.4095/291753>
- Inazaki T (2004) High resolution reflection surveying at paved areas using S-wave type land streamer. *Explor Geophys* 35:1–6. <https://doi.org/10.1071/EG04001>
- International Code Council (ICC) 2015 International Building Code: Washington, D.C., International Code Council Governmental Affairs Office, <https://codes.iccsafe.org/content/IBC2015>. Accessed 01 June 2021
- Jakosky JJ (1950) *Exploration geophysics*. Trija Publishing, Los Angeles
- Jackson F, Molnar S, Ghofrani H, Atkinson GM, Cassidy JF, Assatourians K (2017) Ground motions of the December 2015 M 4.7 Vancouver Island, earthquake: attenuation and site response. *Bull Seismol Soc Am* 107:2903–2916. <https://doi.org/10.1785/0120170071>
- Khasheshi Banab K, Kolaj M, Motazedian D, Sivathayalan S, Hunter JA, Crow HL, Pugin AJM, Brooks GR, Pyne M (2012) Seismic site response analysis for Ottawa, Canada: a comprehensive study using measurements and numerical simulations. *Bull Seismol Soc Am* 102:1976–1993. <https://doi.org/10.1785/0120110248>
- Knapp RW, Steeples DW (1986a) High-resolution common-depth-point reflection profiling: instrumentation. *Geophysics* 51:276–282. <https://doi.org/10.1190/1.1442088>
- Knapp RW, Steeples DW (1986b) High-resolution common-depth-point reflection profiling: field acquisition parameter design. *Geophysics* 51:283–294, *Geophysics* 51:1519 (Errata), and *Geophysics* 51:2011 (Discussion) and 2012 (Reply). <https://doi.org/10.1190/1.1442088>
- Maries G, Ahokangas E, Mäkinen J, Pasanen A, Malehmir A (2017) Interlobate esker architecture and related hydrogeological features derived from a combination of high-resolution reflection seismics and refraction tomography, Virttaankangas, SW-Finland. *Hydrogeol J* 25:829–845. <https://doi.org/10.1007/s10040-016-1513-9>
- Matsubara Y, Yamamoto M, Nobuoka D, Kaida Y (2002) High-resolution shallow seismic reflection using a portable S-wave vibrator. In *Proceedings: Society of Exploration Geophysicists Annual Meeting, Expanded Technical Program Abstracts with Biographies* 21:1618–1621. <https://doi.org/10.1190/1.1816982>
- Miller RD, Pullan SE, Waldner JS, Haeni FP (1986) Field comparisons of shallow seismic sources. *Geophysics* 51:2057–2072. <https://doi.org/10.1190/1.1442061>
- Miller RD, Pullan SE, Steeples DW, Hunter JA (1992) Field comparison of shallow seismic sources near Chino, California. *Geophysics* 57:693–709. <https://doi.org/10.1190/1.1443283>
- Miller RD, Pullan SE, Steeples DW, Hunter JA (1994) Field comparison of shallow P-wave seismic sources near Houston, Texas. *Geophysics* 59:1713–1728. <https://doi.org/10.1190/1.1443558>
- Mooney HM (1984) *Handbook of engineering geophysics, v1, seismic*. Bison Instruments Inc., Minneapolis
- Motazedian D, Hunter JA (2008) Development of an NEHRP map for the Orleans suburb of Ottawa, Ontario. *Can Geotech J* 45:1180–1188. <https://doi.org/10.1139/T08-051>
- Motazedian D, Torabi H, Hunter JA, Crow H, Pyne M (2020) *Seismic Site Period Studies for Nonlinear Soil*

- in the City of Ottawa, Canada; *J Soil Dyn Earthq Eng*, 136. <https://doi.org/10.1016/j.soildyn.2020.106205>
- Musgrave AW (1967) Seismic refraction prospecting. Society of Exploration Geophysicists, Tulsa. <https://doi.org/10.1190/1.9781560802679.fm>
- National Research Council (NRC) 2010 National Building Code of Canada 2010, Volume 1, Division B, Part 4. <https://doi.org/10.4224/40001268>
- Nettleton LL (1940) Geophysical Prospecting for Oil. McGraw-Hill, New York
- Odom JK, Stephenson WJ, Williams RA (2010) Multi-source, high-resolution seismic-reflection imaging of Meeman Shelby fault and possible tectonic model for a Joiner Ridge structure in the upper Mississippi embayment region. *Seismol Res Lett* 81:647–660. <https://doi.org/10.1785/gssrl.81.4.647>
- Palmer D (1988) Refraction seismics: The lateral resolution of structure and seismic velocity. In: Helbig K, Treitel S (eds) *The handbook of geophysical exploration*, Section 1: Seismic Exploration, vol. 13. Geophysical Press, London.
- Pugin AJ-M, Larson TH, Sargent SL, McBride JH, Bexfield CE (2004) Near-surface mapping using SH-wave and P-wave seismic land-streamer data acquisition in Illinois, U.S. *Leading Edge* 23:677–682. <https://doi.org/10.1190/1.1776740>
- Pugin AJ-M, Sargent SL, Hunt L (2006) SH and P-wave seismic reflection using landstreamers to map shallow features and porosity characteristics in Illinois. In *Proceedings: Symposium on the Application of Geophysics to Engineering and Environmental Problems*, Seattle, WA, Environmental and Engineering Geophysical Society, pp 1094–1109. <https://doi.org/10.3997/2214-4609-pdb.181.113>
- Pugin AJ-M, Hunter JA, Motazedian D, Brooks GR, Khareshi-Banab K (2007) An application of shear wave reflection landstreamer technology to soil response of earthquake shaking in an urban area, Ottawa, Ontario. In *Proceedings: Symposium on the Application of Geophysics to Engineering and Environmental Problems*, Denver, CO, Environmental and Engineering Geophysical Society, pp 885–896. <https://doi.org/10.3997/2214-4609-pdb.179.0885-896>
- Pugin AJ-M, Pullan SE, Hunter JA (2009) Multicomponent high-resolution seismic reflection profiling. *Lead Edge* 28:1248–1261. <https://doi.org/10.1190/1.3249782>
- Pugin AJ-M, Pullan SE, Hunter JA (2010) Update on recent observations in multi-component seismic reflection profiling. In *Proceedings: Symposium on the Application of Geophysics to Environmental and Engineering Problems*, Keystone, CO, Environmental and Engineering Geophysical Society, pp 607–614. <https://doi.org/10.3997/2214-4609-pdb.175.SAGEEP070>
- Pugin AJ-M, Brewer K, Cartwright T, Pullan SE, Perret D, Crow HL, Hunter JA (2013) Near surface S-wave seismic reflection profiling – new approaches and insights. *First Break* 31:49–60. <https://doi.org/10.3997/1365-2397.2013005>
- Pugin AJ-M, Yilmaz Ö (2019) Optimum source-receiver orientations to capture PP, PS, SP, and SS reflected wave modes. *Lead Edge* 38:45–52. <https://doi.org/10.1190/tle38010045.1>
- Pugin AJ-M, Brewer K, Cartwright T, Sargent SL (2019) Detection of tunnels and boulders using shallow SH-SH reflected seismic waves. *Lead Edge* 38:436–444. <https://doi.org/10.1190/tle38060436.1>
- Pugin AJ-M, Brewer K, Cartwright T, Dietiker B (2020) Ultra-high frequency reflections using an electromagnetic driven seismic vibrator. In *Proceedings: SEG Technical Program Expanded Abstracts 2020*. Society of Exploration Geophysicists, pp 3447–3451. <https://doi.org/10.1190/segam2020-3422219.1>
- Pullan SE, Hunter JA (1987) Application of the “optimum offset” shallow reflection technique in the Fraser delta, British Columbia. In *Proceedings: 57th Annual Meeting of the Society of Exploration Geophysicists*, New Orleans, pp 244–246. <https://doi.org/10.1190/1.1891891>
- Pullan SE, Jol HM, Gagné RM, Hunter JA (1989) Compilation of high resolution “optimum offset” shallow seismic reflection profiles from the southern Fraser River delta, British Columbia. Geological Survey of Canada, Open File 1992. <https://doi.org/10.4095/130592>
- Pullan SE, Hunter JA (1999) Land-based shallow seismic methods. In: Gilbert R (ed) *A handbook of geophysical techniques for geomorphic and environmental research* (Chapter 3). Geological Survey of Canada, Open File 3731, pp 31–55. <https://doi.org/10.4095/210370>
- Pullan SE, Pugin AJ-M, Hunter JA, Brooks GR (2011) Mapping disturbed ground using compressional and shear wave reflection sections. In *Proceedings: Symposium on the Application of Geophysics to Engineering and Environmental Problems*, Charleston, SC, Environmental and Engineering Geophysical Society. <https://doi.org/10.3997/2214-4609-pdb.247.67>
- Pullan SE, Hunter JA, Harris JB, Crow H, Pugin AJ-M (2015) Shear wave reflection techniques for hazard studies. In: Hunter JA, Crow HL (eds) *Shear Wave Velocity Measurement Guidelines for Canadian Seismic Site Characterization in Soil and Rock*. Geological Survey of Canada, Earth Science Sector, General Information Product 110 e, p.34–47. <https://doi.org/10.4095/297314>
- Rabbel W (2006) Seismic methods. In: Kirsch R (ed) *Groundwater geophysics: a tool for hydrogeology*. Springer, Heidelberg, Germany, pp 23–83
- SEG Technical Standards Committee (2017) SEG-Y_r2.0: SEG-Y revision 2.0 Data Exchange format. Society of Exploration Geophysicists. https://seg.org/Portals/0/SEG/News%20and%20Resources/Technical%20Standards/seg_y_rev2_0-mar2017.pdf. Accessed 03 November 2020
- Sheehan JR, Doll WE, Mandell WA (2005) An evaluation of methods and available software for seismic refraction tomography analysis. *J Environ Eng Geophys* 10:21–34. <https://doi.org/10.2113/JEEG10.1.21>
- Steeple DW (1998) Special Issue: shallow seismic reflection section – Introduction. *Geophysics* 63:1210–1212. <https://doi.org/10.1190/1.1444421>
- Steeple DW (2005) Shallow seismic methods. In: Rubin Y, Hubbard SS (eds) *HydroGeophysics Water Science and Technology Library* 50:215–251. https://doi.org/10.1007/1-4020-3102-5_8
- Steeple DW, Miller RD (1990) Seismic reflection methods applied to engineering, environmental and groundwater problems. In: Ward SA (ed) *Geotechnical and Environmental Geophysics*, v.1. Society of Exploration Geophysics, pp 1–29. <https://doi.org/10.4133/1.2921807>

- Steeple DW, Miller RD (1998) Avoiding pitfalls in shallow seismic reflection surveys. *Geophysics* 63:1213–1224. <https://doi.org/10.1190/1.1444422>
- Stephenson WJ, Williams RA, Odum JK, Worley DM (2007) Miscellaneous high-resolution seismic imaging investigations in Salt Lake and Utah Valleys for earthquake hazards. U.S. Geological Survey Open-File Report 2007–1152. <https://doi.org/10.3133/ofr20071152>
- Stumpel H, Kahler S, Meissner R, Milkereit B (1984) The use of seismic shear waves and compressional waves for lithological problems of shallow sediments. *Geophys Prospect* 32:662–675. <https://doi.org/10.1111/j.1365-2478.1984.tb01712.x>
- Telford WM, Geldart LP, Sheriff RE (1990) *Applied Geophysics*. Cambridge University Press, New York
- Truskowski M, Warner J, Clark J, Tisoncik D (2004) Fault and fracture system delineation of bedrock aquifer. *Society of Exploration Geophysicists* 23:1393–1396 (extended abstract). <https://doi.org/10.1190/1.1843298>
- van der Veen M, Green AG (1998) Landstreamer for shallow seismic data acquisition: Evaluation of gimbal-mounted geophones. *Geophysics* 63:1408–1413. <https://doi.org/10.1190/1.1444442>
- van der Veen M, Bunes HA, Bueker F, Green AG (2000) Field comparison of high-frequency seismic sources for imaging shallow (10–250 m) structures. *J Environ Eng Geophys* 5:39–56. <https://doi.org/10.4133/JEEG5.2.39>
- van der Veen M, Spitzer R, Green AG, Wild P (2001) Design and application of a towed landstreamer for cost-effective 2D and pseudo-3D shallow seismic data acquisition. *Geophysics* 66:482–500. <https://doi.org/10.1190/1.1444939>
- Wang Z, Madin IP, Woolery EW (2003) Shallow SH-wave seismic investigation of the Mt. Angel Fault, northwest Oregon, USA. In: McBride JH, Stephenson WJ (eds) *Contributions of High Resolution Geophysics to Understanding Neotectonic and Seismic Hazards, Tectonophysics* (special issue) 368:105–117. [https://doi.org/10.1016/S0040-1951\(03\)00153-7](https://doi.org/10.1016/S0040-1951(03)00153-7)
- Widess MB (1973) How thin is a thin bed? *Geophysics* 38:1176–1180. <https://doi.org/10.1190/1.1440403>
- Williams RA, Odum JK, Stephenson WJ, Herrmann RB (2007) Shallow P- and S-wave velocities and site resonances in the St. Louis region, Missouri-Illinois. *Earthq Spectra* 23:711–726. <https://doi.org/10.1193/1.2753548>
- Williams RA, Stephenson WJ, Frankel AD, Odum JK (1999) Surface seismic measurements of near-surface P- and S-wave seismic velocities at earthquake recording stations, Seattle, Washington. *Earthq Spectra* 15:565–584. <https://doi.org/10.1193/1.1586059>
- Williams RA, Stephenson WJ, Odum JK, Worley DM (1996) Shallow P- and S-wave velocities at eleven aftershock recording stations of the Northridge Earthquake, San Fernando Valley, California. U.S. Geological Survey Open-File Report 96–261. <https://doi.org/10.3133/ofr96261>
- Williams RA, Stephenson WJ, Odum JK, Worley DM (2003a) Comparison of P- and S-wave velocity profiles from surface seismic refraction/reflection and downhole data. In: McBride JH, Stephenson WJ (eds) *Contributions of High Resolution Geophysics to Understanding Neotectonic and Seismic Hazards, Tectonophysics* (special issue) 368:71–88. [https://doi.org/10.1016/S0040-1951\(03\)00151-3](https://doi.org/10.1016/S0040-1951(03)00151-3)
- Williams RA, Wood S, Stephenson WJ, Odum JK, Mermonte ME, Street R, Worley DM (2003b) Surface Seismic Refraction/Reflection Measurement Determinations of Potential Site Resonances and the Areal Uniformity of NEHRP Site Class D in Memphis, Tennessee. *Earthq Spectra* 19:159–189. <https://doi.org/10.1193/1.1543161>
- Woolery EW, Street RL (2002) Quaternary fault reactivation in the Fluorspar Area Fault Complex of Western Kentucky: Evidence from shallow SH-wave reflection profiles. *Seismol Res Lett* 73:628–639. <https://doi.org/10.1785/gssrl.73.5.628>
- Woolery EW, Street RL, Wang Z, Harris JB (1993) Near-surface deformation in the New Madrid seismic zone as imaged by high resolution SH-wave seismic methods. *Geophys Res Lett* 20:1615–1618. <https://doi.org/10.1029/93GL01658>
- Woolery EW, Wang Z, Street RL, Harris JB (1996) A P- and SH-wave seismic reflection investigation of the Kentucky Bend Scarp in the New Madrid Seismic Zone. *Seismol Res Lett* 67:67–74. <https://doi.org/10.1785/gssrl.67.2.67>
- Xia J, Miller RD, Park CB, Wightman E, Nigbor R (2002) A pitfall in shallow shear-wave refraction surveying. *J Appl Geophys* 51:1–9. [https://doi.org/10.1016/S0926-9851\(02\)00197-0](https://doi.org/10.1016/S0926-9851(02)00197-0)
- Zoeppritz K (1919) Erdbebenwellen VII. VIIb. Über Reflexion und Durchgang seismischer Wellen durch Unstetigkeitsflächen. *Nachrichten von der Königlichen Gesellschaft der Wissenschaften zu Göttingen. Mathematisch-physikalische Klasse*, pp 66–84.

Publisher's note Springer Nature remains neutral with regard to jurisdictional claims in published maps and institutional affiliations.